DYNAMICS SIMULATION OF PYRO ACTUATED 'BALL LOCK' SEPARATION SYSTEM FOR MICRO-SATELLITES TO EVALUATE RELEASE SHOCK.

S. Somanath

Project Manager, Vehicle Engineering & Launch Service Management, PSLV Project, Vikram Sarabhai Space Centre, Trivandrum-695547, India, e-mail: sssnath@hotmail.com, sssnath@rediffmail.com

V. K. Krishnan Kutty

Head, Upper Staging Section, Aerospace Mechanisms Group, Vikram Sarabhai Space Centre, Trivandrum, India.

E. J. Francis

Deputy Project Director, Product Assurance, PSLV Project, Vikram Sarabhai Space Centre, Trivandrum, India

ABSTRACT

Micro-satellite separation systems based on 'Ball Lock' release mechanism developed by ISRO for deploying micro-satellites up to 150 kg mass has been successfully used in PSLV. Three varieties of such designs have been realised and qualified. They are designated as IBL230, IBL298 and IBL358. IBL stands for **I**SRO **B**all **L**ock and the number stands for the interface diameter in mm. The system functions by releasing a preloaded ball locked joint between two rings by rotating a ball retainer ring using pyro assisted thrusters. This system is characterised by good joint stiffness, lightweight construction, tuneable jettisoning velocity, debris free actuation and redundancy in initiation. The system generates low release shock. To reduce the release shock further for sensitive spacecraft applications, the shock sources needs to be identified and suitable methods for attenuation to be chosen. The difficulty in identifying the contribution of shock from various sources was due to lack of complete understanding of system dynamics. Experimental verification was attempted to understand the dynamics of the release operations. Dynamic model of this system is generated for complete understanding of the release function and to quantify the impact forces that generate the shock.

A dynamics model of the IBL298 system was generated. The pyro thrusters are the source of energy for release function. It is powered by ISRO standard cartridge with squib based electrical initiation. The firing of the cartridge generates pressure inside the thruster, which moves a piston and rotates the retainer ring. The pressure time relationship used for modelling is generated from the test data from a closed bomb test and used in the simulation by applying constituent equations. The system is modelled using second order dynamical equations. This model is made to capture the multiple contact losses that are likely to occur between the thruster and the lug of the ring during the movement. Magnitudes of the forces are evaluated when the thrusters are actuated simultaneously. The analysis was also carried out for off nominal conditions like one thruster not working or working with a delay. The modelling was carried out using MATLAB and solved using the odesuits.

Matching with the ground test results the model parameters were firmed up. The simulation results showed that the impact forces generated at the stopper are very high. The model was further used to study the feasibility of reducing the shock, incorporating shock attenuation systems.

Nomenclature

p_p	: Peak pressure in closed bomb	V_i	: Instantaneous volume in pyrothruster
p_t	: Pressure in pyrothruster unexpanded	V_1	: Initial volume inside pyrothruster
$p_{f_{1,2}}$	: Final pressure in thrusters after expansion	V_b	: Volume of the closed bomb
p_c	: Pressure in closed bomb	V_c	: Volume of the pyro charge
t	: Time	M	: Mass of spacecraft
t_p	: Peak pressure occurrence time	m_p	: Mass of piston
$t_{d_{1,2}}$	: Delay time in initiation of pyrothruster	m_c	: Mass of pyro charge
$d_{p_{1,2}}$	: Displacement of piston 1 & 2	m_x	: Mass of pyro charge consumed
$d_{r_{1,2}}$	: Displacement of retainer lug 1 & 2	F_{rp}	: Frictional force in piston
d_m	: Displacement of spacecraft	F_{rr}	: Frictional force in retainer ring
$v_{p_{1,2}}$	: Velocity of piston 1 & 2	$F_{sp_{1,2}}$	: Piston stop force
$v_{r_{1,2}}$	: Velocity of retainer lug 1 & 2	$F_{sr_{1,2}}$	: Retainer ring stop force
		$F_{ps_{1,2}}$	: Pin shear force on piston

$F_{pr_{1,2}}$: Pin shear force on retainer lug

K_s : Jettisoning spring stiffness

k_{pr} : Stiffness of piston & retainer lug

k_{rs} : Stiffness of retainer ring & stopper

k_{pc} : Stiffness of piston & case

A : Area of piston

C_r : Kinetic coefficient of restitution

R : Radius of piston contact on lug

R_b : Radius at which balls are positioned

R_r : Radius at which friction acts on retainer

R_l : Radial position of shear pins on retainer lug

N : Number of jettisoning springs

r : Radius of balls

J : Polar MI of retainer ring

n : Index of polytropic expansion

s_p : Maximum stroke of piston

s_r : Maximum stroke of retainer ring lug

S_s : Maximum stroke of springs

0_l : Distance of ball contact on retainer ring from edge of hole

1. INTRODUCTION

'Ball Lock' based separation systems were developed for micro-satellites of mass class up to 150 kg to be flown in Polar Satellite Launch Vehicle (PSLV). These systems generate low release shock at the satellite interface. Typical measured acceleration response and the Shock Response Spectrum (SRS) at the interface of the system with the satellite is shown in Fig: 1&2. For sensitive satellite applications, further reduction of the release shock was planned. Functional tests were conducted with instrumentation to demonstrate various configurations. These tests were in limited numbers and hence could not simulate all the parameters that govern the magnitude of the shock. The available measurements on the release dynamics showed that very short time period is involved in the release (less than 1ms). The difficulty with the measurements was due to the small dimensions and time periods. In the standard system no shock attenuation systems have been employed so as to make the system simple.

To understand the release dynamics, a mathematical model of the IBL298 system is generated. The objective of this model is to simulate and predict the dynamics of the separation system and to understand the release dynamics under various functional conditions. From the computation of the impact forces, the sources of release shock can be identified. In this model, the results of the simulation are compared with the available test data and the model parameters are firmed up. The reduction of shock is addressed for use of this system for spacecrafts with sensitive equipments. After identifying the shock sources, some simple shock attenuation devices are suggested. Simulation studies were carried out with typical shock attenuation systems.

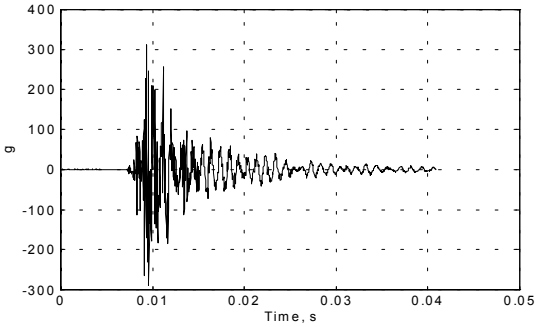

Fig: 1 Response measured on the satellite interface

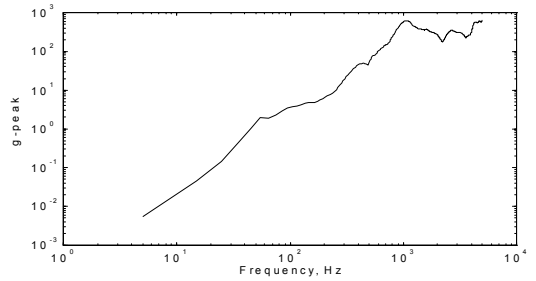

Fig: 2 SRS of the measured response

2. SYSTEM DESCRIPTION

The configuration of the separation system is shown in Fig: 3. The system consists of three rings. The fore-end ring interfaces with the satellite. The aft end ring is attached to the launch vehicle deck. These rings are held together using a ball lock and pre-loaded radially using a retainer ring which provides the required joint stiffness. The retainer ring is locked in position using two shear screws attached to the stopper bracket. For releasing the system, the retainer ring is to be rotated overcoming the redial pre-load and friction and shearing the pins through a fixed angle. The required angle is reached when the lug of the retainer ring makes contact with the stopper mounted on the aft ring. The holes on the retainer ring aligns with the balls in the aft ring and jettisoning springs cause the separation of the for end ring. The configuration of the piston and the retainer lug, which is of interest in this model, is shown in Fig:4. There are two pyro thrusters mounted on a bracket attached to the aft ring keeping a small gap from the retainer ring lug. The pyro thrusters are mounted so as not to make contact with the stopper lug and retainer ring at the end of the stroke. This is to prevent the impact of the piston on the lug at the end of the stroke. There are eight sets of compressed springs providing jettisoning energy for the spacecraft. The springs react on the fore end ring, which forms a part of the spacecraft after separation.

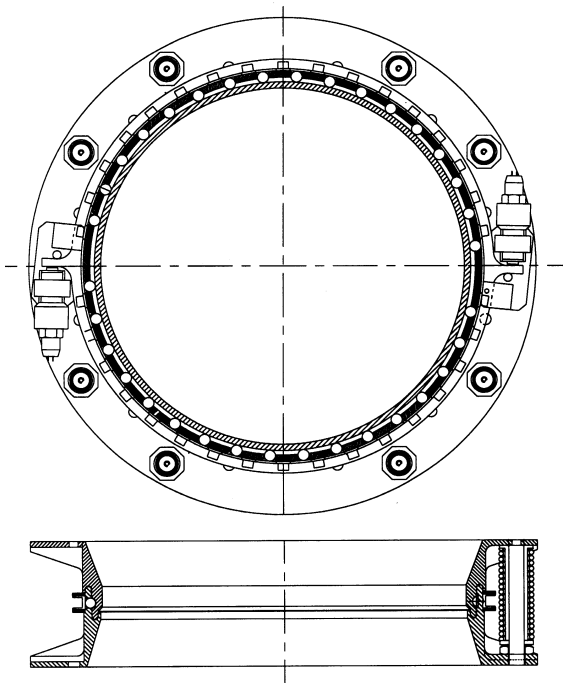

Fig: 3 Configuration of the IBL298 system

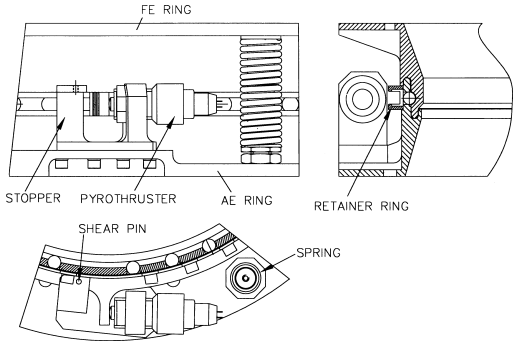

Fig: 4 Details at the pyrothruster mounting.

3. DESCRIPTION OF THE MODEL

Formulation of various elements of the model is discussed in this section.

Pressure-Time trace

The ISRO standard cartridge is used for producing the pyro thruster. The design is made to generate an upper bound force at the end of a pre-defined stroke. The stroke corresponds to the angular rotation required by the retainer ring. The energy of the combustion products from the cartridge is used for driving the piston. The piston is provided with shaft O-rings for sealing purpose. The cartridge is tested in a closed bomb with 10 cc volume. In the closed bomb test, the pressure rise and decay are captured using pressure pickup. One of the typical test curves is shown in Fig: 5. The peak pressure is reached in about 33 ms from the start of pressure rise. A simulation data is generated from the test data with peak pressure occurring at various times lower than the test data. This is by assuming that the burn rate is augmented with increase in chamber pressure.

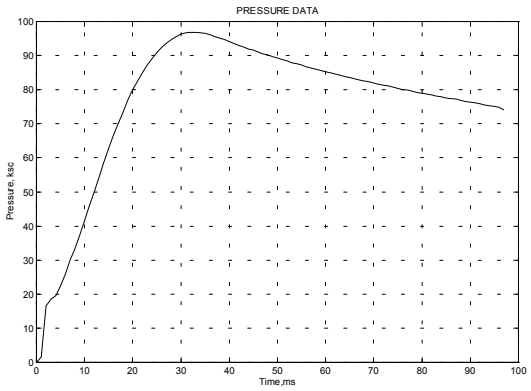

Fig: 5 Closed bomb test data

The pressure drop due to heat loss to surrounding is reflected in the decay curve. This is not considered to change considerably, as the time periods involved are small. In the pyro-thruster, the initial cavity volume is computed from the geometry. The simulation data is used to compute the initial pressure in the reduced cavity. The volume generated by the movement of the piston is used for computing the pressure during the expansion process. The expansion process is assumed to be polytropic [Ref: 1]. The combustion of the explosive charge is assumed to be linearly regressive with the complete combustion occurring at the peak pressure time. Based on the displacement of the piston at any time the pressure is computed. A burn rate parameter is defined as:

$$b = \frac{m_c}{\left(t_p - t_d\right)}$$

This is used to compute the amount of charge burnt at any time given by the expression.

$$m_x = b\left(t - t_d\right)$$

The volume generated in the chamber is

$$V_i = V_1 + \left(\frac{V_c}{m_c}\right) m_x$$

The pressure in the chamber is given by

$$p_t = p_c \left(\frac{V_b}{V_i}\right)^n$$

The pressure when expanded to the chamber generated by the piston displacement is given by:

$$p_{f_{1,2}} = \frac{p_t . V_i^{\,n}}{\left(V_i + A.d_p\right)^n}$$

The pressure computed using the above mentioned process is quite high as compared to the closed bomb test even for the same rate of combustion assumed. This high pressure will cause the combustion process to accelerate by a factor, which is to be evaluated [Ref: 2]. Since there is uncertainty on the rate of combustion, different times for peak pressure occurrence are used for parametric study

Friction in piston and retainer ring

A fixed value friction in the piston based on internal pressure and O-ring specification is used. This frictional force is acting in the opposite direction to the motion of the piston if the velocity is above a breakout level. Friction in the retainer ring motion is evaluated using hydraulic actuators. The force at the start of the movement of the retainer ring is taken as the fixed value of coulomb friction. This frictional force is made to act in the direction opposite to the motion of the retainer ring if the velocity is above a breakout level and till the balls in the system are aligned with the holes on retainer ring.

Shearing of pins

The locking pins in the piston and retainer rings are to be sheared off with the movement. The shearing of the pin is assumed to take place till the piston or the retainer ring travels through a distance equal to the pin diameter. The area remaining to be sheared is computed from the geometry and multiplied with the material shear strength to get the shear forces.

Contact force between piston and retainer ring lug

It is assumed that the force transfer takes place through the collision(s) of piston and the retainer ring lug. It is required to know the position and velocities of both piston and lug to predict a collision condition and compute the contact force. The conditions for the direction of velocities, and displacements of piston and retainer ring lug are evaluated to predict a collision scenario. This can be expressed as the following condition:

$$v_p - v_r > 0 \,\&\, d_r - d_p < 0$$

The contact forces are dependant on the stiffness of the elements participating in the collision process. The stiffness of the piston and retainer ring lug was evaluated using geometry and material properties. The equivalent stiffness is evaluated as:

$$k_{pr} = \frac{k_p . k_r}{\left(k_p + k_r\right)}$$

The force of contact is evaluated as

$$F_c = C_r k_{pr} \left| d_r - d_p \right|$$

The term in the mode bracket corresponds to the combined deflection of the piston and lug. This is applicable if the piston and the retainer are moving towards each other. After the collision or during subsequent separation, the elastic forces developed between them are released. The kinetic coefficient of restitution corresponding to the material combination is applied to compute the forces using the above expression during the separation process.

Stop forces in the piston

The stop force is developed due to collision between the moving piston and stationary case at the end of the stroke. The stiffness of the case and the piston heads are computed and equivalent stiffness is used for computation of the force.

$$F_{sp} = C_r k_{pc} \left(d_p - s_p \right)$$

After the velocity is brought to zero and in subsequent separation, appropriate value of kinetic coefficient of restitution is applied to compute the forces as the system relieves the elastic forces.

Stop force between retainer ring lug and stopper

The stop force is developed due to collision between the moving retainer ring and stationary stopper at the end of the stroke. The stiffness of the lug of retainer and the stopper are computed and equivalent stiffness is used for computation of the force.

$$F_{sr} = C_r k_{rs} \left(d_r - s_r \right)$$

Force during collision and separation is computed in the same way as in case of piston stop force.

Spring force & movement of the fore-end ring

The two rings of the system are forced to separate by the jettisoning springs. The force by the springs are given by:

$$F_{Spring} = K_s \left(S_s - d_m \right)$$

Until the retainer ring rotates to the start of the uncovering balls by holes on the ring, the spring force is zero. The spring force is zero after the completion of the spring stroke. The equation of motion of the spacecraft mass is given by the following expression:

$$M\ddot{y} = NF_{Spring}$$

Where y is the displacement of the Fore-end ring.

Force exerted by balls on retainer ring to assist rotation

The balls exert radial pressure on the retainer ring due to the separation force between the rings. The preloads disappear when the holes in the retainer ring starts uncovering. The radial force due the springs will make the balls move outward due to the assistance provided by the moving fore-end ring. The balls exert forces on the edge of the holes of the retainer ring. The configuration of the ball and the forces acting during release is shown in Fig: 6.

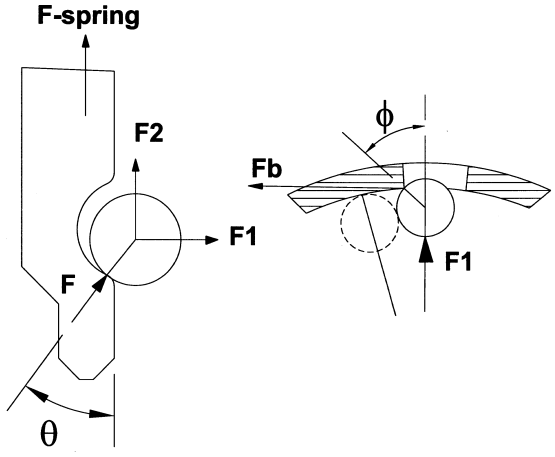

Fig: 6 Forces on the ball during release

The force exerted by the balls on the retainer ring is zero when F_{Spring} is zero or when the retainer rings moves enough to complete the uncovering of the balls. From the geometry the following angles are determined to evaluate the component of the spring force acting on the retainer ring.

$$\theta = Cos^{-1}\left(Cos\left(\pi/4\right) - \left(d_m/r\right)\right)$$

$$\phi = Sin^{-1}\left(\frac{d_r - o_l}{r}\right)$$

$$F_b = \frac{N}{4} F_{Spring} Sin(2\theta).Sin(2\phi)$$

This force will be zero if $d_m \geq r\left(1 - Cos\left(\pi/4\right)\right)$

Movement of piston

The piston mass is accelerated by the expanding gas in the cavity. Instantaneous pressure is used to compute the force acting on the piston mass. The shear screw is to be sheared off before movement. The governing equation is the following:

$$m_p \ddot{x}_1 = p_{f_1} A + F_{rp_1} - F_{ps_1} - F_{c_1} - F_{sp_1}$$

Where, x is the displacement of the piston. The subscript 1 stands for the first pyro-thruster and 2 for the second one. There is a shear pin, which has to be sheared off to start the movement of the piston. The shear force for the pin F_p is computed by considering of the area of pin remaining multiplied by the shear strength of the material.

Movement of retainer ring

The retainer ring rotates by the action of torque developed due to various forces applied at different radii. The torque on the retainer ring is expressed as follows:

$$T_1 = RF_{c_1} + R_b F_b + R_r F_{rr} - R_l F_{pr_1} \;\&$$

$$T_2 = RF_{c_2} - R_l F_{sr_2}$$

$$T = T_1 + T_2$$

This computation will result in negative values of torque. To overcome this $T = 0$ if $T < 0$ and net torque is given by

$$T_{net} = T - R(F_{sr_1} + F_{sr_2})$$

if $T > 0$

The equation of motion of the retainer ring is given by

$$J\ddot{\alpha} = T_{net}$$

Where, α is the angular displacement of the retainer ring. The displacement is computed as;

$$d_r = \alpha R$$

4. Simulation Programme

MATLAB programmes were written for the above-defined model. The ten variables to be evaluated are displacements and velocities of pistons, retainer ring lugs, and the spacecraft. The second order equations describing the movement of piston, retainer rig and spacecraft were converted to first order expressions. Functions were written for the evaluation of pyrothruster chamber pressure, frictional forces, contact forces, stop forces, force from the balls on retainer, spring force and shear force of pins. The integration of the differential equations was carried out using **ode23** function of MATLAB. The parameters to be varied in the simulations were the peak pressure occurrence time and delay time between the pyrothruster and total simulation time.

5. Results form the ground tests

In the ground tests, measurements were made to get the ignition delay between the pyro thrusters and strain on the retainer ring lug. The strain data identified the events of contact between the piston and the stopper. The fire current delay information is given in Fig: 7, which is about 1.5 ms. The strain signature on the retainer ring lug is given in Fig: 8. The initial portion of the strain shows the start of the movement of the retainer ring and the hitting on the stopper lug. The total travel duration is less than one milliseconds. The result indicate that only one pyro thruster is really active for the release of the system, and the other thrusters moves through and stopped by the retainer lug, with out participating in the release function.

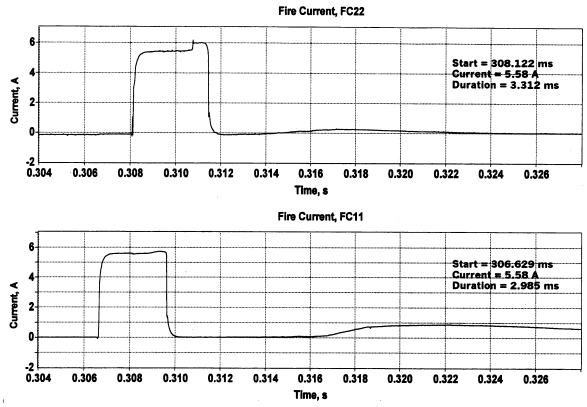

Fig: 7 Fire currents

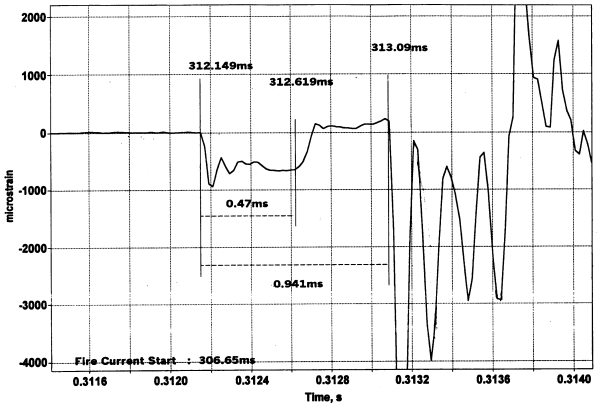

Fig: 8 Portions of strain data showing contact time

6. Simulation Results

The displacement and velocities of the piston and retainer rings are evaluated from simulations. Corresponding to the peak pressure time of 1ms, the results are shown in Fig: 9. To identify the set of results that match with the ground tests the peak pressure time is varied. The simulation results were matching with the ground test results when the peak pressure reaching time is 3 ms. The results are shown in Fig: 10. The retainer ring is moving with slightly higher velocity than the piston and loosing contact intermittently. The retainer ring collides with the stopper and bounces back and makes multiple contacts with the piston. The contact forces, stop forces, and friction forces are shown in Fig: 11. The duration of the impact at the stopper is of the order of 0.001ms. The pressure developed with in the pyro-thruster chamber is given in Fig: 12. The force exerted by the balls, and the spring forces are also shown in Fig: 12. The spring force is almost constant as the movement of the Fore-end ring is small. The retainer ring after the collision with the stopper moves back and hits the piston and pushes it backwards. Due to the prevailing pressure inside the pyro thruster; the retainer ring is moved back to the release position

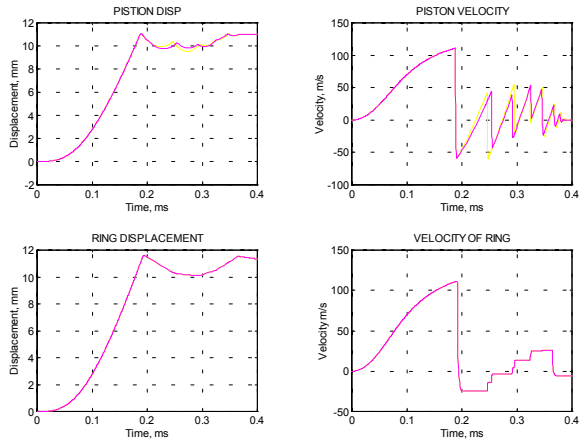

Fig: 9 Simulation results (peak pressure at 1ms)

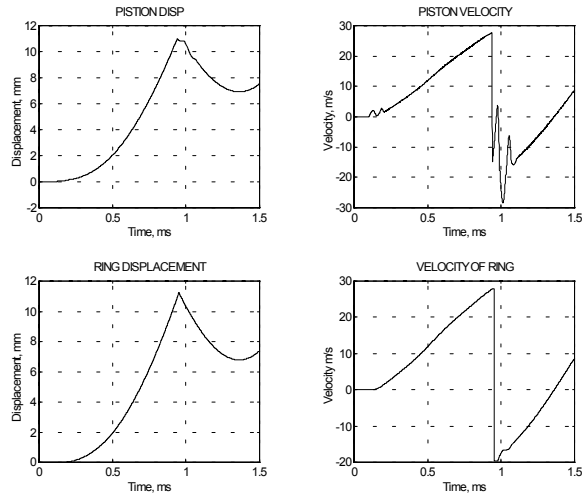

Fig: 10 Simulation results (peak pressure at 3ms)

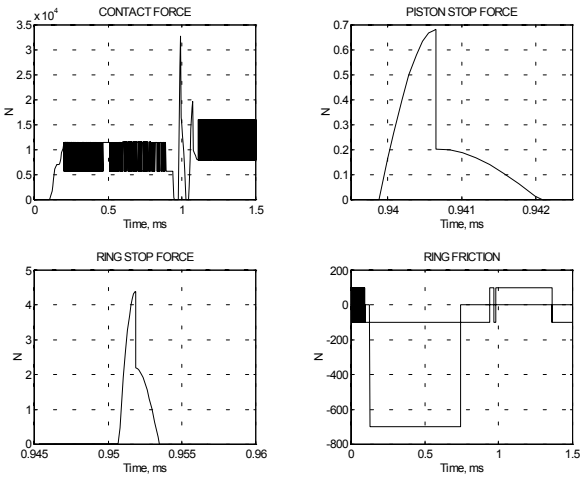

Fig: 11 Contact forces, stop forces and friction

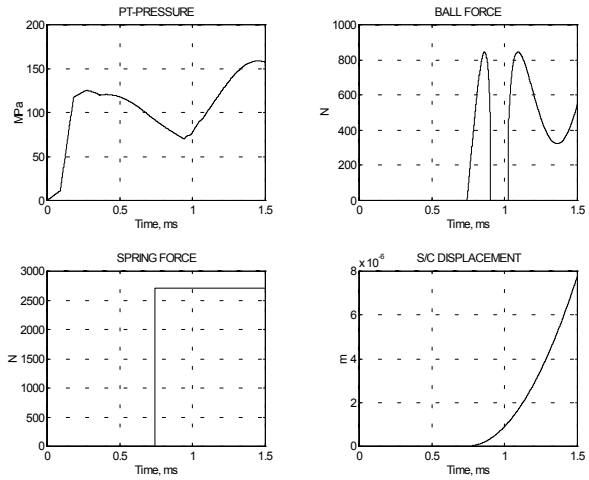

Fig: 12 Pressure inside pyro-thruster etc.

If both the pyro thrusters are acting simultaneously, the release will be accomplished faster and the impact forces are higher. The simulation result is shown in Fig:13.

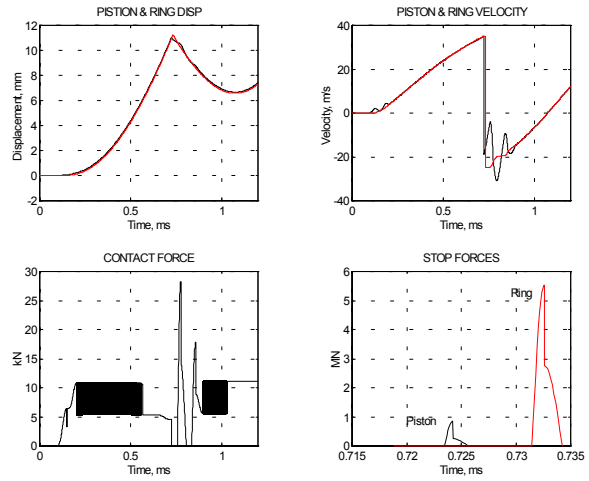

Fig: 13 Both pyro-thrusters acting simultaneously.

It is seen that the release is completed in about a millisecond, while the combustion continues up to 3 ms, indicating excess charge in the pyro-thruster. Simulation was carried out with single thruster having reduced charge (90mg) and results are shown in Fig: 14. It was also noted that with the reduced charge, the peak pressure inside the thruster chamber is not reduced appreciably. The impact forces are reduced only marginally. Hence it was concluded that reduction in charge might not alter the release dynamics or resultant shock appreciably.

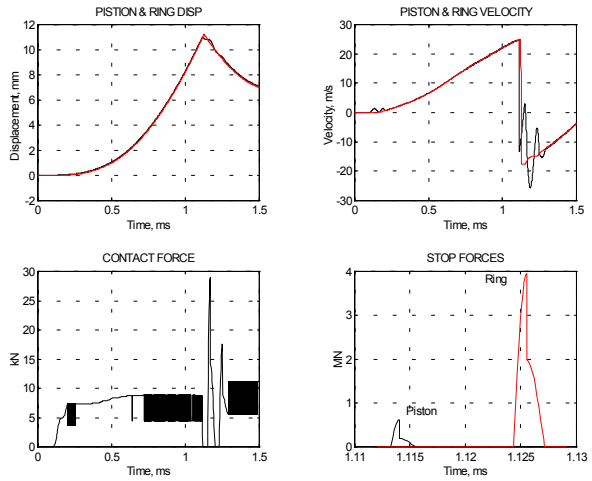

Fig: 14 Results with reduced pyro charge

7. Shock attenuation systems

The major parameter contributing the shock generated is the velocities achieved by the retainer ring and piston. The impact of the retainer ring on the stopper and the impact of the piston within the pyro thruster are major source of shock excitations. The deceleration of the retainer ring while hitting can be made slower with a soft or crushable material positioned at the impacting interface. Materials like lead, crushable materials like honeycomb dimpled structural element etc. can be used for this purpose. The alignment requirement between the retainer ring and the balls to cause the release is to be ensured even with this system. This requires that the compression / crushing shall be limited to a fixed stroke length and the retainer should be stopped at a hard reference interface at the stopper. Hence the entire energy absorption is not feasible. Possible configurations of the system with this constraint are shown in Fig: 15. Simulation carried out with various damping materials appropriately modelled showed that the impact forces could be reduced by about 25%. The impact damper stiffness is iteratively chosen to cause the velocity change in the retainer ring as shown in Fig:16.

The piston impacting inside the body of the pyro-thruster also generate shock. Feasibility of reduction of this impact force was not investigated in detail. The contribution in shock generated by the piston hitting the body is small which is evident from the magnitude of the impact force compared to the retainer ring hitting the stopper.

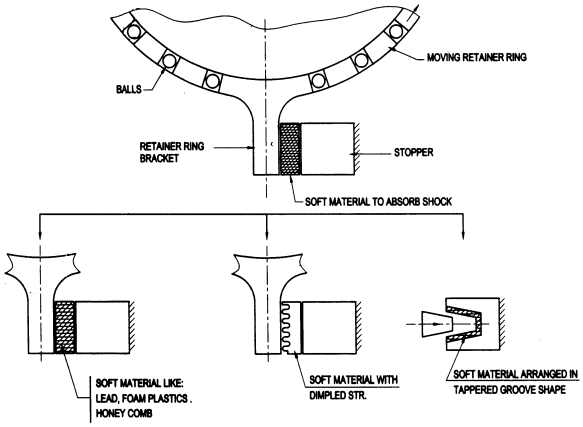

Fig: 15 Options for shock attenuation systems

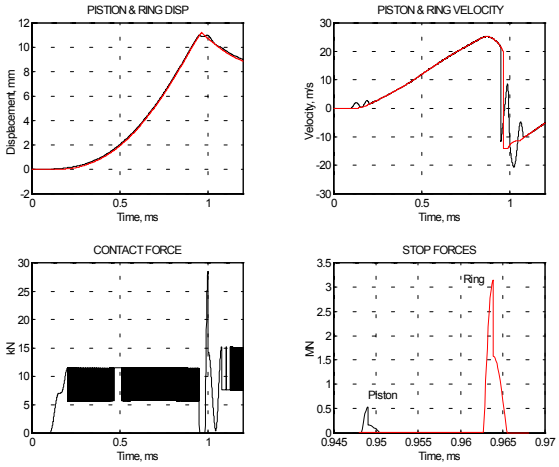

Fig: 16 Simulation results with impact damper

8. Conclusions

The complete model of the 'Ball Lock' separation system is generated. The simulations have been carried out to match with the limited results obtained from the ground tests. The simulations yielded the velocity and displacement histories of the retainer ring lug and the pistons. The impact forces between the retainer lug/stopper and the piston/pyro thruster case are

generated. This quantified the shock generated in the system. With the simultaneous initiation of the second pyro thruster the minimum release time and the maximum impact forces are evaluated. Simulations carried out with reduced charge in the pyro thruster showed that the shock could be marginally reduced. The shock attenuation systems could be introduced in the system for reducing the impact forces further. The model was further utilised to evaluate shock attenuation systems.

9. Assumptions & limitations

The model is generated with the experimental pressure-time data from pyro thruster closed bomb tests. The data corresponds to a few tests and the variation in the pressure history with possible variations in the actual charge loaded is not accounted. The index of expansion is based on an earlier reference and is to be validated. The rate of combustion of the charge is assumed to be regressive, which is hypothesised from the test data. The augmentation of the burn rate with pressure is not fully understood. This is applied as a constant rate defined only by the time of occurrence of peak pressure. The frictional forces are evaluated using hydraulic tests. There are variations in different assemblies, which is of the order of 20 to 30%. The shearing of the lock pin is assumed to be pure shear with no bending, which can induce higher loads. The contact and impact forces are evaluated assuming the materials to be hookean, with no permanent set occurring due to high contact stresses.

The kinetic coefficient of restitution is based on the reference data and no evaluation is separately done for the material and geometry combination. The retainer ring is assumed to be rigid with out flexibility between the lugs. If the retainer ring is considered flexible, there will be difference in the impact timings between both locations on account of this.

10. Acknowledgements

The authors wish to acknowledge the support of the design and development team of the IBL systems at ISRO and the testing team who provided valuable data for this study. The authors acknowledge the suggestions given by Mr. A Subramoniam, who heads the mechanisms team in VSSC. We also acknowledge the support of the Project Director, PSLV and Director, VSSC who permitted us to pursue this study and publish the findings.

11. References

1. Jung-hua Kuo & S. Golstein; 'Dynamic Analysis of NASA Standard Initiator Driven Pin Puller', AIAA-93-2066, 29th Joint Propulsion Conference, 1993.
2. Keith A Gonthier & Joseph M Powers; 'Formulation, Prediction, and Sensitivity Analysis of a Pyrotechnically Actuated Pin Puller Model', Journal of Propulsion and Power, Vol.10, No. 4, July-Aug, 1994.
3. S Barret & W J Kacena; 'Methods of Attenuating Pyrotechnic Shock'.
4. Michael W Mosher; 'Reduction of Shock Response Spectra Using Various Types of Shock Isolation Mounts', Taylor Devices, Inc.
5. E. Hornung & H. Oery; "Pyrotechnic Shock Loads Test Evaluation, Equipment Protection", IAF-97-I.2.06
6. NASA/TM-1998-206621; 'Statistical Analysis of a Large Sample Size Pyro-shock Test Data Set'.
7. W. J. Stronge; "Impact Mechanics", Cambridge University Press, 2000.